

Laboratory-based assessment of the Underwater Laser Scanner ULi

Ellen Heffner¹, Annika L. Walter¹, Annette Scheider¹, Harald Sternberg¹

¹ Dept. of Hydrography and Geodesy, HafenCity University Hamburg, Germany –
(ellen.heffner, annika.walter, annette.scheider, harald.sternberg)@hcu-hamburg.de

Keywords: Underwater Laser Scanning, Laboratory Environment, Turbidity, Böhler-Star, Sphere Fitting.

Abstract

Optical measurement methods are widely used for precise and high-resolution underwater monitoring applications, however, remain limited in range as they are strongly affected by visibility. Through enhancements in laser technology, green LiDAR systems expand the range in the underwater domain under favourable conditions. The Underwater LiDAR System (ULi), recently developed by the Fraunhofer Institute for Physical Measurement Techniques (IPM), is a Time-of-Flight (ToF) laser scanner optimized for underwater operation. This paper assesses the actual performance of ULi under varying environmental conditions in controlled laboratory setups. We present the results of static scans on different test objects like a Böhler-Star, spheres and metal plates at different distances and varying turbidity levels. Through repetitive range measurements on a metal plate range precision of ULi is evaluated to be 1.95 mm and ULi achieves a mean relative range accuracy of 6.01 mm. Additionally, we demonstrate that objects like small shells and water plants can be clearly identified in low turbid water.

1. Introduction and Motivation

The global underwater infrastructure is increasing and along with it the demand for precise and high-resolution monitoring solutions. Optical underwater measurement methods are superior to established acoustic technologies as echosounders in terms of resolution and accuracy due to shorter wavelengths of light in comparison to sound waves. However, optical sensing methods are strongly affected by visibility under water and therewith remain limited in range due to water turbidity. Through enhancements in laser technology, green LiDAR systems expand the range in the underwater domain under favourable conditions (Massot-Campos and Oliver-Codina, 2015). While airborne bathymetric laser systems became popular over the last decades and are meanwhile an established surveying technique for shallow water domains as many publications show (e.g. Awadallah et al., 2023; Mandlbürger et al., 2020; Schwarz et al., 2019), the performance and usability of underwater laser scanners is still to be investigated.

Most underwater laser scanners on the market are triangulation scanners, utilizing a laser projector emitting a laser line and camera for detecting precise object shapes (Niemweyer et al., 2019; Bleier et al., 2019; Hildebrandt et al., 2008). Only few publications show first insights into underwater Time-of-Flight (ToF) laser scanners (e.g. Werner et al., 2023; Maccarone et al., 2023; Imaki et al., 2016) as it is a comparably new field of laser scanning application (Filisetti et al., 2018). Currently, there are only two commercial systems on the market available (3DatDepth, 2025; Fraunhofer IPM, 2024). The recently developed Underwater LiDAR System (ULi) by the Fraunhofer Institute for Physical Measurement Techniques (IPM) is such a ToF-scanner using a green pulsed laser with 532 nm wavelength, optimized for underwater operation (Werner et al., 2023). ULi offers a high level-of-detail potential for monitoring applications and, by making use of a full wave form analysis, it can potentially be used for plant and macro fauna detection in the context of habitat mapping.

To assess and evaluate the actual performance of ULi under varying environmental conditions, we performed static measurements in water tanks under controlled laboratory conditions. Our investigations use established terrestrial laser scanner targets as a Böhler-Star and evaluation procedures as

the approximation of known shapes as spheres and planes (Kersten et al., 2008).

The presented study addresses the following research questions:

- What is the maximum measurement range of ULi to resolve a Böhler-Star under varying water turbidity?
- Which range precision and relative accuracy can ULi achieve throughout repetitive measurements?
- How clearly can ULi capture structures for object recognition?

2. Methods

In this chapter we describe the used methodology, instrumentation and experimental setups for the investigation of the raised research questions.

2.1 Underwater LiDAR System ULi

The underwater laser scanner ULi is ToF laser scanner optimized for underwater sampling. According to the manufacturer, ULi reaches scanning ranges of several tens of meters and up to twice the secchi depth with a sub-millimetre precision in clear waters (Fraunhofer IPM, 2024). With a sampling frequency of up to 100,000 points per second and a field of view (FoV) of 44 °, the system allows capturing very dense point clouds in static or dynamic applications. By making use of two rotating wedge prisms, the laser scan pattern can be set to linear, circular or planar for capturing the entire FoV. The laser scanner can be operated in two different laser modes, being laser class 2M for the filtered adjustment mode and laser class 3B in the stronger unfiltered mode. Since laser radiation from laser class 3B is dangerous for human eyes and skin, appropriate laser safety measures like laser goggles must be taken during respective measurements.

ULi consists of a scanning unit in a waterproof cylindrical housing with a depth rating of 300 m and a separate processing unit outside of the water to power the scanner and connect ULi via Ethernet connection to a laptop or PC. Over a graphical User Interface the operator can adjust the scanning settings and access the scanned data. Time synchronization is realised over a Precise Time Protocol (PTP) Timeserver. Figure 1 illustrates the scanner unit fixed in a water tank on a constructed ITEM profile

mounting for static scans. During all measurements we recorded parallelly the water turbidity with a fluorometer on either an AML LGR-3 Probe or a Valeport Probe, which can be seen as well in Figure 1.



Figure 1. The Underwater LiDAR System ULi developed by Fraunhofer IPM in a static setup mounted on an ITEM profile construction to hang it in the water tanks. A Valeport turbidity probe is hanging in the water behind ULi to record water properties.

So far, we tested ULi in primarily static operation in smaller water tanks with freshwater to assess its performance on different materials. We showed that brighter and smoother surfaces (e.g. a white coated steel plate or a white resopal plate) – just as for terrestrial scanners – are scanned with higher precision in comparison to dark, matt and rough surfaces as wood or rusty metal plates (Walter et al., 2025a). Additionally, ULi has been mounted on the Survey Vessel “DVocean” for first insights into dynamic real-world applications (Walter et al., 2025b; Scheider et al., 2025). However, as turbidity in the Elbe river during the first test surveys did not allow satisfying scanning results, it seemed obvious to test the performance of ULi under varying turbidity levels in controlled laboratory conditions.

2.2 Tank measurements

The measurements for this study have been conducted in two laboratory water tanks with varying water conditions. In the laboratory facilities of the Institute of Mechanics and Ocean Engineering (MUM) from the Technical University Hamburg (TUHH) measurements are carried out in clear freshwater with an average turbidity of 0.0 NTU, while in the large-scale recirculating flume of the Federal Waterways Engineering and Research Institute (BAW) in Hamburg measurements with varying turbidity from 0.9 to 4.6 NTU are carried out.

The freshwater tank is a 15 m long, 1.5 m wide and 1.6 m deep glass basin, filled to a water level of 1.2 m. As the tank has a wave generator build in, the maximum achievable distance between scanner and targets is 8 m.

The recirculating flume is a 220 m long closed-circuit flume with a straight rectangular test section which is about 70 m long and 1.5 m wide. The water level is filled up to 1.5 m and flow can be generated with a bow thruster outside of the test section. Additionally, depending on the flow and amount of dissolved particles in the water, the turbidity in the tank can be steered. Over a length of 8 m a movable traverse is mounted over the tank. This traverse can be steered automatically with millimetre precision over the water to achieve reproducible setups of instruments hanging from the traverse into the water. Both tanks are shown in Figure 2.

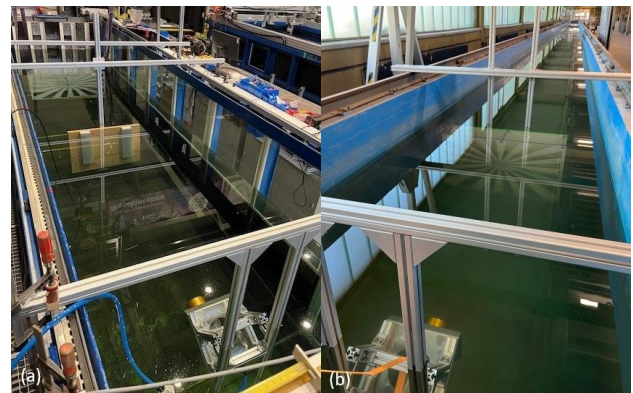


Figure 2. The two tanks used for the experiments.
(a) Freshwater basin at the Institute of Mechanics and Ocean Engineering (MUM) at Technical University Hamburg (TUHH); (b) Recirculating flume with adjustable water turbidity at Federal Waterways Engineering and Research Institute (BAW) in Hamburg.

To evaluate the resolution capability of the underwater laser scanner under varying water conditions, 85 static scans of a Böhler-Star have been performed. A Böhler-Star is a typical calibration target for determining the spatial resolution of a laser scanner. First described by Böhler et al. (2003), it is meanwhile a common method for terrestrial laser scanner evaluations (e.g. Jost et al., 2020; Schmitz et al., 2020) but have not been used in the underwater domain so far. Our newly constructed, water-resistant Böhler-Star has an overall size of 1 m x 1 m and consist of 16 cut out wedges in the front panel beginning in the middle of the star with an opening angle of 11.25°. A more detailed description can be found in Walter et al. (2025b). The distance between both panels is adjustable and has been set to 24.9 cm for the here presented scans. A series of static Böhler-Star scans have each been carried out at water turbidity of 0 NTU, 0.9 NTU, 2.4 NTU and 4.6 NTU, while the distance between ULi and Böhler-Star has been step-wise increased by half or one meter up to the maximum measurement range when the star was not able to be identified in the scan data anymore. To judge the range precision and accuracy, repetitive scans on a plate with small defined variations in the distance to the scanner are performed. A white coated metal plate, where best reflectivity can be expected, is fixed under the movable traverse for these measurements. The traverse is moved in centimetre and millimetre steps for each ten steps towards and away from the scanner with repetitive scans at each location. To assess the shape capture capability of the underwater laser scanner, a white plastic spheres with a diameter of 10 cm is scanned at varying turbidity levels and distances. Moreover, sceneries with several objects of different size, material and surface texture (metal, plastic, shells and plants) are measured to evaluate the multi-echo detection performance of the scanner as well as its object recognition ability.

2.3 LiDAR data processing

The scanned data is processed in Pulsalyzer and CloudCompare. The proprietary software Pulsalyzer is used to review the recorded waveforms and convert them into 3D point clouds. An example of a full waveform analysis with multi-echo detection is displayed in Figure 3.

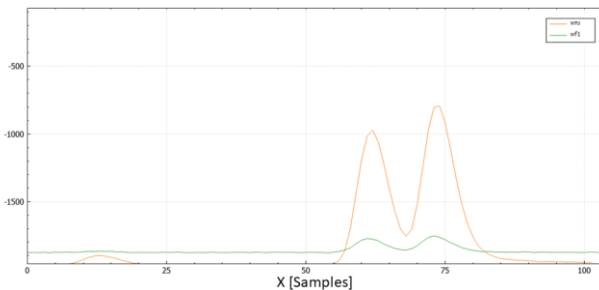


Figure 3. Example of full waveform analysis with two detected echos (peaks) in one recorded pulse, displayed in the Processing Software Pulsalyzer with the green line being the rough channel and the orange line being the sensitive channel of ULi.

The data is then exported into .las files for further processing and analysis in the opensource software CloudCompare. Most presented results within this paper are derived from unfiltered point cloud data, while for the plane and sphere fitting analysis we performed manual segmentation of the object of interest out of the entire point cloud first. The sphere fitting was performed with Matlab scripts, while plane fitting and most other analysis was done in CloudCompare.

3. Results

The performance of ULi strongly varies with the prevailing water turbidity. Thus, results are presented according to the different water conditions and scanned targets.

3.1 Böhler-Star scans in freshwater

In the freshwater tank with turbidity values of 0.0 NTU, ULi shows excellent results in the weaker 2M laser class mode. Despite the occurrence of typical scanning artefacts as e.g. mixed-pixels, comet tails and strong edge-effects (which are further discussed in chapter 3.5), ULi completely resolves the rays of the Böhler-Star independent of the scanning distance and different distances between the front and rear panel of the Böhler-Star (Walter et al., 2025). The arc elements of the Böhler-Star measure 2.95 mm at the inner circle and are sharply captured up to the maximum possible range within the tank (8 m between ULi and Böhler-Star) as can be seen in Figure 4.

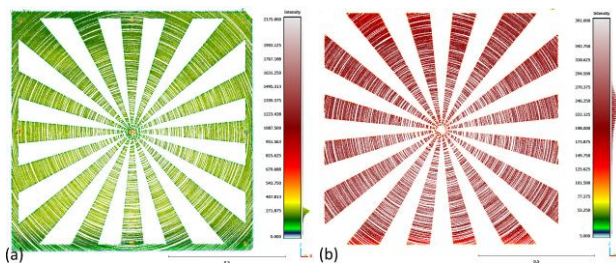


Figure 4. Point cloud of Böhler-Star scan in freshwater at 8 m distance in 2M laser mode of (a) front and (b) rear panel coloured by intensity.

3.2 Böhler-Star scans in low turbid water

In low turbid water with a measured mean turbidity of 0.9 NTU, scanning resolution show similar results at close ranges as in freshwater. However, the larger the distance between ULi and target becomes, the more scattering of the point cloud at the object and general more noise can be observed. In the turbid water tank, the maximum distance between ULi and Böhler-Star can be increased. The example in Figure 5 shows that at 17 m distance the Star can still be fully resolved in 3B laser mode, however not with same intensity and point density compared to the closer range results. We observed, that the longer the distance, the less intense are the captured reflections and the sparser becomes the point cloud of detected points.

At the maximum distance of 18 m between Böhler-Star and scanner, only the front panel of the Böhler-Star can partly be recognized in the data (see Figure 6a). The rear panel is not visible in the point cloud anymore.

In the weaker 2M laser class mode the Böhler-Star is still captured with front and rear panel at 8 m distance, however, at 9 m distance as well only the front panel is partly captured (see Figure 6b). As can be seen in Figure 6, the screws of the Böhler-Star are higher reflective than the rest of the front panel, and due to more turbidity close to the bottom of the tank caused by the movement of the Böhler-Star the lower half of the Star is less captured than the upper part.

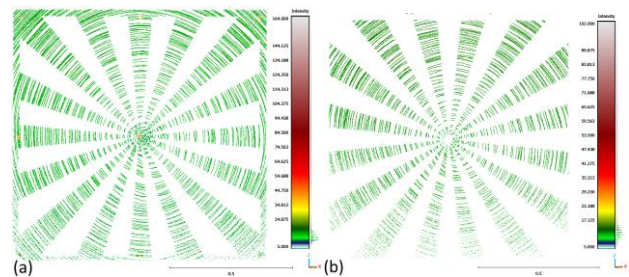


Figure 5. Point cloud of Böhler-Star scan in low turbid water at 17 m distance in 3B laser mode of (a) front and (b) rear panel coloured by intensity.

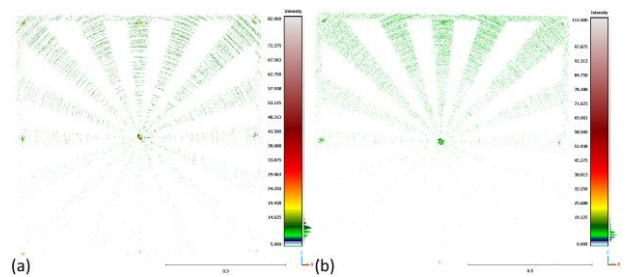


Figure 6. Point cloud of Böhler-Star (only front panel) at maximum reached distances in low turbid water (0.9 NTU) coloured by intensity (a) at 18 m distance in 3B laser mode; (b) at 9 m distance in 2M laser mode.

3.3 Böhler-Star scans in moderate turbid water (2.4 NTU)

The measurements in moderate turbid water with an average measured turbidity of 2.4 NTU show a different picture: the maximum scan distance with full resolution of the Böhler-Star is determined at 2.5 m with the 2M laser mode and 4.5 m with the stronger 3B laser mode. At 5 m distance the scanner still captures the front panel of the Böhler-Star, but the rear panel is not detected anymore. Both examples of the scanned front panels at the maximum reached distances are shown in Figure 7.

We observed the same behaviour as in low turbid water: if ULi fully captures the front panel, the arc elements of the Böhler-Star are resolved. However, intensity of the reflected beams drastically decreases with increasing scanning range and increasing turbidity, and the number of detected points decreases. At a certain distance about twice the Secchi-depth, mixed-pixels between front and rear panel increase, edge effects at the edges of the cut-out wedges become stronger and the rear panel is only merely captured by single points. The edge effects can be seen in the lateral view of the Böhler-Star in Figure 9c in chapter 3.5.

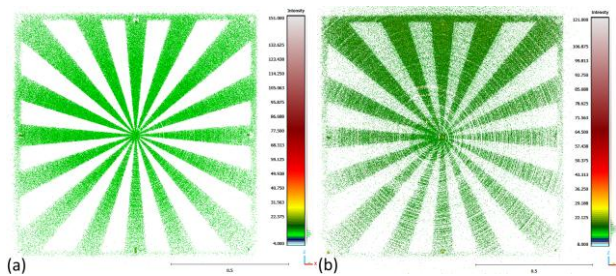


Figure 7. Point cloud of Böhler-Star (only front panel) at maximum reached distances in moderate turbid water (2.4 NTU) coloured by intensity (a) at 2.5 m distance in 2M laser mode; (b) at 5 m distance in 3B laser mode.

3.4 Böhler-Star scans in turbid water (4.6 NTU)

In turbid water with an average measured turbidity of 4.6 NTU and a secchi-depth of 1 m the measurements show expected limited results. The front panel of the Böhler-Star can be captured at 1 m distance, but not with same resolution as under clearer water conditions (see Figure 8). At 1.4 m distance, the front panel is still fully captured, but at twice the secchi-depth (2 m distance) the scanner merely captures single point reflections, but not enough to identify the front panel of the Böhler-Star.

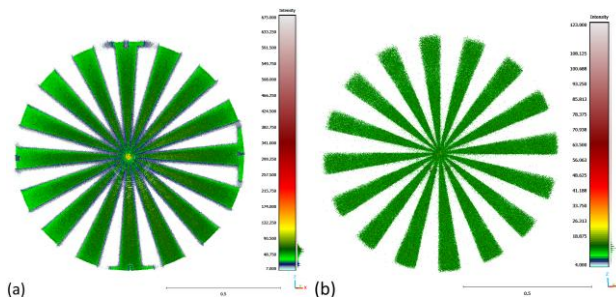


Figure 8. Point cloud of Böhler-Star (only front panel) in turbid water (4.6 NTU) in 2M laser mode coloured by intensity (a) at 1 m distance; (b) at 1.4 m distance.

3.5 Edge effects and noise behaviour

The edge effect and noise behaviour of the scanned data strongly varies with the turbidity level of the water, the used scanner settings (including the operational laser mode) and the distance between scanner and object. In Figure 9 we show the lateral view of the Böhler-Star Scans under different water conditions measured always at 1 m distance from the scanner in 2M laser mode. One can see three typical effects which are already known from terrestrial laser scanners: mixed-pixels (which occur whenever two objects are spatially adjacent in the range direction and one beam cannot distinguish between both surfaces, thus the reflected signal is integrated between both distances); edge effects (which occur at sharp edges when only

a part of the signal is reflected from the target and the edges cause a smearing of the signal, sometimes denoted as comet tails); and a spreading of the scanned data in range direction depending on the scanned surface material.

Figure 9 illustrates that with 24.9 cm distance between front and rear panel the effect of mixed-pixels is barely present in the scanned data. Both panels can be clearly separated from each other in all water turbidity levels. Only at 4.6 NTU (Figure 9d) one can recognize individual mixed-pixel points (in dark blue) between the two panels.

However, one can clearly see the already mentioned edge effects (light blue points), mainly in Figure 9a-c. The edge effects do not occur uniformly, but stronger at the surrounding edges of the panels and at the cut-out Böhler-Star rays. In turbid water of 4.6 NTU, the edge effects are not detectable anymore, they seem to be overlain by the overall spreading and noise of the data at the detected surface of the Böhler-Star panels (see Figure 9d).

One can clearly see that the lateral spreading of the data at both panels strongly increase with increasing turbidity. We measured this distance with the point to point picking tool in CloudCompare and received values from 3 cm lateral spreading of the data at the front panel in freshwater to 7 cm lateral spreading in turbid water (see Table 1). By fitting a plane in the data of the scanned front panels at different turbidity levels one receives with the Root Mean Square (RMS) of the best fit plane a measure for the lateral precision of the scanned data. The plane fitting algorithm results with RMS values from 0.28 cm in fresh water to 0.66 cm in turbid water (see Table 1).

Therewith we can state that when measuring in 2M laser mode the edge effects occur stronger in lower turbidity, while the overall noise and lateral spreading of the data at detected objects increases with increasing turbidity.

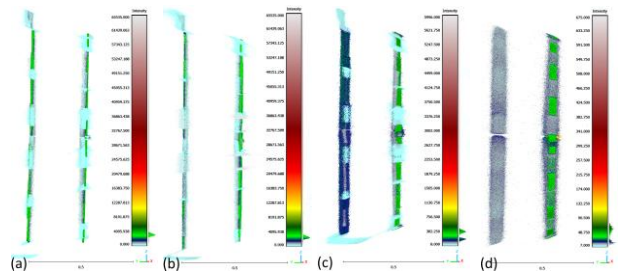


Figure 9. Lateral view of Böhler-Star scans at 1 m distance in (a) freshwater (0.0 NTU); (b) low turbid water (0.9 NTU); (c) moderate turbid water; (d) turbid water (4.5 NTU).

Turbidity of water	Precision at front panel of Böhler-Star	
	Measured spreading of data	RMS of best fit plane
0.0 NTU	3 cm	0.28 cm
0.9 NTU	3 cm	0.29 cm
2.4 NTU	6 cm	0.44 cm
4.6 NTU	7 cm	0.66 cm

Table 1. Precision at front panel of Böhler-Star at 1 m distance in water of different turbidity levels.

In 3B mode the signal-to-noise ratio becomes worse, again depending on the water turbidity level and surfaces of scanned objects. A lot of noise and erroneous reflections can be observed within the water column and multi reflections from objects and side walls due to the limited extent of the tank are

recognized by the scanner in 3B mode in comparison to the 2M mode. An example is shown in Figure 10, where we scanned an underwater scenery with many different objects in low turbid water of 0.9 NTU. In Figure 10a, measured with 2M laser mode, one can distinguish easily between objects, tank walls, tank bottom and water surface and only minor erroneous reflections in the water column and reflections above water surface are visible. In Figure 10b, measured with 3B laser mode, one can barely distinguish between different objects without filtering the data, as the point cloud is overlain by primarily reflections from the water column and multiple side reflections from side walls, water surface and other effects.

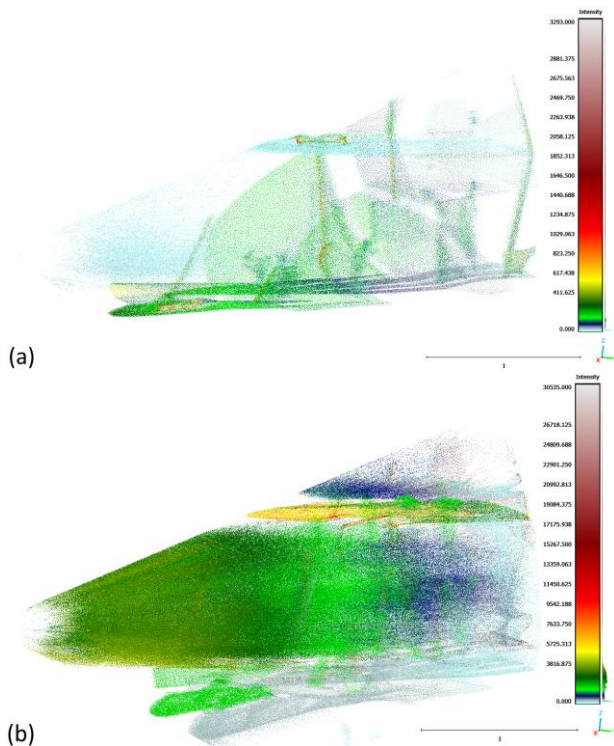


Figure 10. Scenery scan data in low turbid water of 0.9 NTU measured in (a) 2M laser mode; (b) 3B laser mode.

3.6 Range precision and relative accuracy

The relative range measurements on the white coated metal plate operated from the movable traverse are evaluated to judge on range precision and a relative range accuracy of ULi in low turbid water (1.6 NTU). The range precision on the metal plate is again evaluated over the best fit plane RMS. In the experiment series where the metal plate is moved in centimetre steps, the mean best fit plane RMS is calculated to be 2.12 mm. In the experiment series where the metal plate is moved in millimetre steps, the mean best fit plane RMS is calculated to be 1.95 mm.

The relative range accuracy of ULi is evaluated by comparing the calculated mean distances between the fitted planes in the measured data of the metal plate at each location to the true distance which the metal plate has been moved. This bias between calculated and true distance is analysed in the experiment series with centimetre steps and millimetre steps. The results are displayed in Table 2, where the results are additionally separated according to the moving direction of the metal plate away from (forward) and towards (backward) the scanner. We observed that in the experiment series with centimetre steps the relative distance of 1 cm is nicely captured

in the first ten steps moving away from the scanner with the smallest mean bias of only 0.22 mm. However, when measuring the millimetre steps in the same moving direction, ULi measures in two from ten measurements almost double the relative distance and therewith the mean bias from the true distance results in 13.25 mm. In the other moving direction towards the scanner, the data shows better results in the experiment series with millimetre steps. While the mean calculated distance with - 2.23 mm is still too big compared to the true distance of - 1 mm, the mean bias of - 1.23 mm is still smaller than in the experiment series with centimetre steps. Overall, we can state that ULi reaches a relative range accuracy of - 3.37 mm in the experiment series with centimetre steps and in the experiment series with millimetre steps a relative range accuracy of 6.01 mm. Therewith we can show, that ULi is able to capture relative distances with millimetre range accuracy.

Moving direction of plate from scanner	Calculated mean distance	Mean bias from true distance
Forward [cm steps]	1.133 cm	0.022 cm
Backward [cm steps]	- 1.694 cm	- 0.694 cm
Forward [mm steps]	14.25 mm	13.25 mm
Backward [mm steps]	- 2.23 mm	- 1.23 mm

Table 2. Relative range accuracy of ULi in experiment series with repetitive scans on a metal plate moved stepwise away from and towards the scanner.

3.7 Sphere fitting and object recognition

The scanned spheres of 10 cm diameter are analysed in moderate turbid and freshwater. Examples of fitted spheres are visualized in Figure 11. In clear freshwater the scan shows almost no noise, and the sphere fitting derives values of a fitted diameter of 10.26 cm and a standard deviation of 0.11 cm of the sphere in 3 m distance. In low turbid water (1.6 NTU) the scan of the sphere in 2.5 m distance reveals more noise at the sphere surface (fitted diameter of 6.21 cm and a standard deviation of 1.26 cm). However, measured with the 3B laser mode, the edge effects at the side of the sphere become very strong in the direction towards the scanner, but the scanned surface of the sphere shows less noise (see Figure 12). The most accurate result in fitting a sphere is achieved in the 3B laser mode scanned data after filtering the noise at the edges by manual segmentation: the fitted diameter results in 10.80 cm with a standard deviation of 0.06 cm. Generally, the diameter of the sphere is overestimated slightly both in freshwater as well as in low turbid water, a reason could be that the reference diameter of the sphere has been measured in air and that the sphere eventually expands under water, as it is an unconventional plastic sphere with two drilled holes which fills with water as soon as it is submerged.

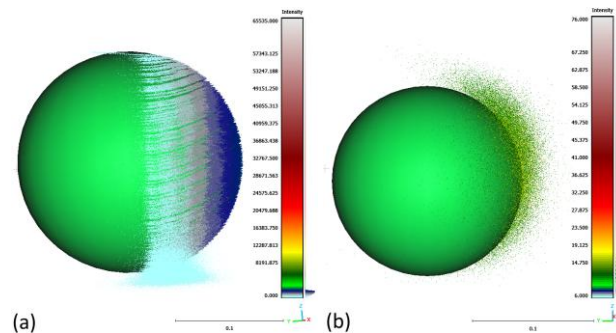


Figure 11. Example of fitted sphere in scanned data (a) in freshwater; (b) in low turbid water (1.6 NTU).

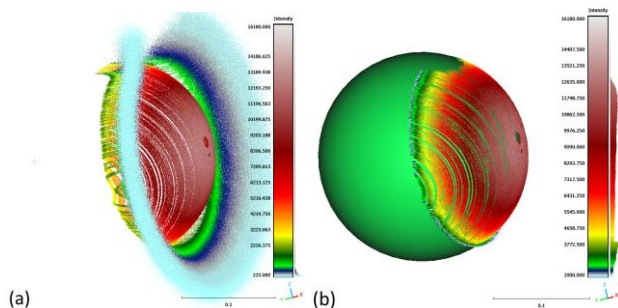


Figure 12. Example of scanned data in low turbid water (1.6 NTU) in 3B laser mode showing (a) the strong edge effects and (b) the fitted sphere after manual segmentation.

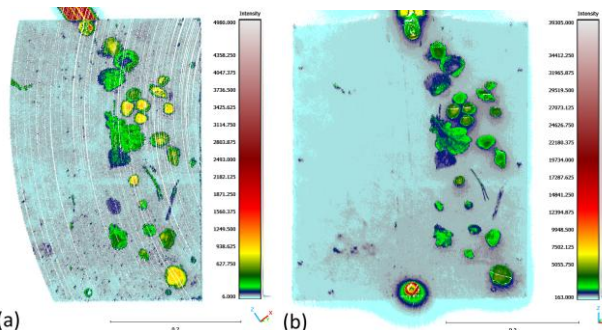


Figure 13. Point cloud of scanned shells on a wooden plate coloured by intensity (a) in freshwater (0 NTU); (b) in moderate turbid water (2.4 NTU).

The scenery scan data with shells, wood, metal and plants are moreover analysed to further investigate the object recognition ability of ULi. Examples of point clouds with scanned shells in the size of some centimetres, glued on a wooden plate, are shown in Figure 13, while examples of a point cloud from a scenery scan including aquarium water plants of about 15 cm height are shown in Figure 14a and Figure 14b. We assert that small shells in the range of centimetres as well as water plants can be clearly identified in static scans at 2.5 m scanning distance in moderate turbid water (2.4 NTU). To evaluate the multi-echo detection performance of the scanner the point cloud with water plants is coloured by echo return number in Figure 14c. All points coloured in blue are retrieved from the first returned echo. One can clearly see that in the vicinity around the shadowed area by the water plants the point cloud is derived out of the second returned echo (light green areas), however, one cannot see areas of higher echo return numbers (would be coloured in red). The expectation that ULi could capture points behind the water plants' leaves by making use of the multi-echo detection ability is therewith not yet confirmed.

4. Conclusion

The presented results in this paper show the high potential of the Underwater LiDAR System ULi for monitoring applications as well as plant and macro fauna detection in the context of habitat mapping. We assessed and evaluated the actual performance of ULi under varying environmental conditions by performing static measurements in water tanks under controlled laboratory conditions with varying turbidity levels. The results of static scans on different test objects like the Böhler-Star at different distances and varying turbidity levels show, that ULi is able to resolve a Böhler-Star with arc elements of 2.95 mm at the inner circle in low turbid water (0.9 NTU) at a maximum measurement range of 18 m, in moderate turbid water (2.4 NTU) at 5 m and in turbid water (4.6 NTU) at 1.4 m maximum measurement range. Through repetitive range measurements on a metal plate, range precision of ULi is evaluated to be 1.95 mm and ULi achieves a mean relative range accuracy of 6.01 mm. A white sphere of 10 cm diameter can be captured well in moderate turbid water at 2.5 m distance in 3B laser mode, where the fitted diameter results in 10.80 cm with a standard deviation of 0.06 cm. Additionally, we demonstrated that objects like small shells and water plants can be clearly identified in moderate and low turbid water. Therewith, we conclude that ULi is eligible to capture small structures for object recognition in the underwater environment. Further investigations on the multi-echo capability of ULi need to be performed, especially in the context of scanning underwater plants, as so far only a maximum of two return echos per beam have been achieved.

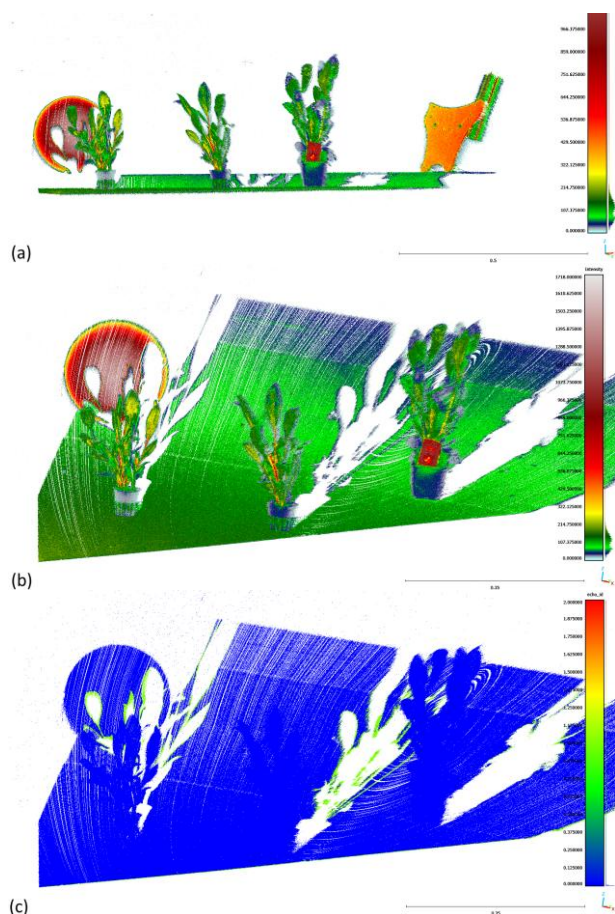


Figure 14. Scenery scan data of plants. (a) front view of plants and sphere coloured by intensity; (b) oblique view of plants and sphere coloured by intensity; (c) oblique view of plants and sphere coloured by echo return number.

Acknowledgements

This work was supported by, and experiments were carried out at the Federal Waterways Engineering and Research Institute (BAW) in Hamburg and the Institute of Mechanics and Ocean Engineering (MUM) of the Technical University Hamburg (TUHH).

References

Awadallah, M. O. M., Malmquist, C., Stickler, M., Alfredsen, K., 2023. Quantitative Evaluation of Bathymetric LiDAR Sensors and Acquisition Approaches in Lærdal River in

- Norway. *Remote Sensing*, 15(1), 263. doi.org/10.3390/rs15010263
- Bleier, M., van der Lucht, J., Nüchter, A., 2019. SCOUT3D – An underwater laser scanning system for mobile mapping, *Int. Arch. Photogramm. Remote Sens. Spatial Inf. Sci.*, XLII-2/W18, 13–18, doi.org/10.5194/isprs-archives-XLII-2-W18-13-2019
- Boehler, W., Vicent, M., Marbs, A., 2003. Investigating laser scanner accuracy. *Proc. XIXth CIPA Symposium*, Antalya, Turkey.
- Fraunhofer IPM, 2024. Underwater LiDAR System. Optical inspection of underwater infra-structure. Long range, high precision 3D mapping. ipm.fraunhofer.de (6 April 2025).
- Filiseti, A., Marouchos, A., Martini, A., Martin, T., Collings, S., 2018. Developments and applications of underwater LiDAR systems in support of marine science. *OCEANS 2018 MTS/IEEE Charleston*, Charleston, SC, USA, 2018, 1-10. doi.org/10.1109/OCEANS.2018.8604547
- Gangelhoff, J., Werner, C. S., Reiterer, A., 2025. Luftgestützte hochaufgelöste Vermessung flacher Gewässer am Beispiel des Rheins. *Journal of applied hydrography*, 130, 36-41. doi.org/10.23784/HN130-05
- Hildebrandt, M., Kerdels, J., Albiez, J., Kirchner, F., 2008. A practical underwater 3D-Lasercanner. *OCEANS 2008, 15-18 September 2008*, Quebec City, QC, Canada. doi.org/10.1109/OCEANS.2008.5151964
- Imaki, M., Ochimizu, Tsuji, H., Kameyama, S., Saito, T., Ishibashi, S., Yoshida, H., 2016. Underwater three-dimensional imaging laser sensor with 120-deg wide-scanning angle using the combination of a dome lens and coaxial optics. *Opt. Eng.*, 56(3), 031212. 10.1117/1.OE.56.3.031212
- Jost, B., Coopmann, D., Kuhlmann, H., Holst, C., 2020. Using the Resolution Capability and the Effective Number of Measurements to Select the "Right" Terrestrial Laser Scanner. *Contributions to INGEO & SIG 2020*, Dubrovnik, Croatia.
- Kersten, T., Mechelke, K., Lindstaedt, M., Sternberg, H., 2008. Geometric Accuracy Investigations of the Latest Terrestrial Laser Scanning Systems. *FIG Working Week 2008, 14-19 June 2008*, Stockholm, Sweden. 421-434
- Maccarone, A., Drummond, K., McCarthy, A., Steinlehner, U. K., Tachella, J., Garcia, D., Pawlikowska, A., Lamb, R. A., Henderson, R. K., McLaughlin, S., Altmann, Y., Buller, G. S., 2023. Submerged single-photon LiDAR imaging sensor used for real-time 3D scene reconstruction in scattering underwater environments. *Opt. Express*, 31, 16690-16708.
- Mandlbürger, G., Pfennigbauer, M., Schwarz, R., Flöry, S., & Nussbaumer, L., 2020. Concept and Performance Evaluation of a Novel UAV-Borne Topo-Bathymetric LiDAR Sensor. *Remote Sensing*, 12(6), 986. doi.org/10.3390/rs12060986
- Massot-Campos, M., Oliver-Codina, G., 2015. Optical Sensors and Methods for Underwater 3D Reconstruction. *Sensors*, 15(12), 31525-31557. doi.org/10.3390/s151229864
- Niemeyer, F., Dolereit, T., Neumann, M., Albiez, J., Vahl, M., Geist, M., 2019. Untersuchungen von optischen Scansystemen zur geometrischen Erfassung von Unterwasserstrukturen. *Hydrographische Nachrichten*, 113, 16-25. doi.org/10.23784/HN113-02
- Scheider, A., Walter, A.L., Heffner, E., Sternberg, H., 2025. Future challenge in the calibration of high-resolution hydrographic multi-sensor systems. *FIG Working Week 2025, 6-10 April 2015*, Brisbane, Australia.
- Schmitz, B., Kuhlmann, H., Holst, C., 2020. Investigating the resolution capability of terrestrial laser scanners and its impact on the effective number of measurements, *ISPRS J. Photogrammetry. Remote Sens.*, 159, 41-52.
- Schwarz, R., Mandlbürger, G., Pfennigbauer, M., Pfeifer, N., 2019. Design and evaluation of a full-wave surface and bottom-detection algorithm for LiDAR bathymetry of very shallow waters. *ISPRS Journal of Photogrammetry and Remote Sensing*, 150, 1-10. doi.org/10.1016/j.isprsjprs.2019.02.002
- Werner, C. S., Gangelhoff, J., Frey, S., Steiger, D., Reiterer, A., 2023. Development of a compact pulsed time-of-flight LiDAR platform for underwater measurements. *The International Hydrographic Review*, 29(2), 200-207. doi.org/10.58440/ihr-29-2-n09
- Walter, A. L., Heffner, E., Scheider, A., Sternberg, H., 2025a. Underwater Laser Scanning: Integration and Testing in different environments. *FIG Working Week 2025, 6-10 April 2015*, Brisbane, Australia.
- Walter, A. L., Heffner, E., Scheider, A., Sternberg, H., 2025b. Underwater Laser Scanning Evaluating the performance of ULI in laboratory environments and presenting first insights from real-world applications. *The International Hydrographic Review*, 31(1), 192-204. doi.org/10.58440/ihr-31-1-n05
- 3DatDepth, 2025. 3D at Depth are developers of the world's first truly deepwater LiDAR. 3datdepth.com/technology/ (26 May 2025).